Available online at www.sciencedirect.com
ScienceDirect
Polymer 48 (2007) 638–651
polymer
www.elsevier.com/locate/polymer

Theoretical study of polymer brushes by a new numerical mean field theory

Georgios Kritikos, Andreas F. Terzis*

Department of Physics, School of Natural Sciences, University of Patras, Rion, GR 26504 Patras, Greece

Received 12 September 2006; received in revised form 16 November 2006; accepted 20 November 2006
Available online 13 December 2006

Abstract

We present a new numerical self-consistent mean field approach in order to investigate poly-disperse polymer brushes dissolved in solvent. In this new method, the polymer segments are contained in a tube filled with solvent, which allow the realization of several configuration of the chain. The tube conformation is developed on a lattice using Kuhn segment, such that the volume of the polymer chain is the same with the one measured experimentally. In order to deal with the depletion layer observed in the volume fraction profile in previous theoretical investigations and obtain more brush-like conformations at high enough concentrations, we introduce a new parameter (disturbed walk parameter), which characterizes the degree of the deviation from the random walk growth. The results show a better description of the brush at high concentrations. Close to the surface, disappearance of the depletion layer was observed. Also we have accomplished the correct description of the brush extension.
© 2006 Elsevier Ltd. All rights reserved.

Keywords: Polymer brush; Self-consistent mean field method

1. Introduction

The polymer brushes are chains anchored by one end to a surface or an interface [1–6]. They are often formed by adsorption from solution, i.e. by bringing a solution containing end functionalized chains into contact with an interacting surface. The ends can either be chemically attached (quite high binding energy [7,8]) or physi-adsorbed [9–11]. The adsorbing, functional end could be a reactive group or the immiscible block of a copolymer [12–19]. Strong overlap among neighboring chains is observed once the distance between grafted points is small compared to the macromolecular chain dimensions. Hence, the chains deform and stretch in the direction perpendicular to the interface.

The numerical self-consistent field theory on a lattice is a powerful method that can describe well polymer brushes [20–23]. The growth of the polymer chain on a lattice allows us to reduce the number of chain conformations while the introduction of the Boltzmann factor (stiffness) [26–30] promotes the more realistic ones. But still the possible configurations give some variations from the volume fraction profile obtained experimentally, especially near the surface. Moreover the good estimation of the total polymer volume fraction in each point of the lattice is not consisted of realistic enough conformations. In the case of numerical self-consistent field (nSCF) methods where the stiffness is introduced through the size of the lattice site (Kuhn segment) the site is full of polymer indicating overestimated density. On the other hand in earlier methods, where the segment density is considered correctly the polymer configuration is limited by the lattice. As a result even though we might obtain satisfactory results in the total volume fraction in a certain point of the solution we cannot have clear estimate about the contribution of each conformation. In order to take advantage of the lattice approximation and also overcome some of its restrictions, we have developed a new approach that permits polymer chain to move in continuum space which is contained in a tube. The tube is a chain of cubic sites, set on a cube lattice. They

* Corresponding author. Tel./fax: +30 2610 997618.
E-mail address: terzis@physics.upatras.gr (A.F. Terzis).

0032-3861/$ - see front matter © 2006 Elsevier Ltd. All rights reserved.
doi:10.1016/j.polymer.2006.11.039

contain polymer segments surrounded by solvent. In this way we can estimate in a more efficient way the contribution to the total volume fraction of each polymer configuration with important statistical weight.

In this work we mainly present the new nSCF method. In Section 2 we give the theoretical formulation and mapping of a real chain on the lattice. In Section 3 we test and compare our new method to predictions from previous nSCF and results from neutron reflectivity (NR) experiments [24,25]. Finally, in Section 5 we end our presentation with conclusions and proposals for future studies.

2. The block self-consistent field model

2.1. Theoretical formulation

We consider a three-dimensional (xyz) lattice of simple structure (usually cubic). The size of each cubic lattice site is equal to the size of a Kuhn (statistical) segment. Each polymeric segment is calculated using the Flory segment introduced in our previous nSCF method [29,30], which is smaller than the Kuhn segment. Hence, in this approach, in the case of polymeric solutions each lattice site contains both polymer and solvent. In this method we can find sites fully occupied by solvent named as solvent blocks. Then, the sites occupied by both polymer and solvent are named as polymer blocks. The macromolecular chain placed on the lattice is the block chain (i.e. a collection of polymer blocks) which contains the polymer chain. In this way the polymer chain is developed in semi-continuum space, since the I, L and V conformations of three successive lattice sites introduced in our previous nSCF method restricts only the block chain. We will refer to this new method as block-nSCF (or bnSCF).

The substrate is placed parallel to the xy-plane; the resulting lattice layers of the block chain (planes parallel to the surface) are numbered consecutively, starting from the layer next to the surface ($z=1$) and ending at a layer ($z=M$) where the presence of the substrate has negligible effect. Each layer is one lattice site thick and contains L lattice sites. Each lattice site has Z neighboring sites, a fraction λ_0 of which lie in the same layer and a fraction λ_1 of which lie in each of the adjacent layers. The coordination number (Z) reflects the point symmetries characterizing the lattice ($Z=6$ for cubic; $\lambda_0=4/6$ and $\lambda_1=1/6$). In order to describe a constant volume system on the lattice, each lattice site must be occupied by exactly one block (polymer or empty solvent block). The block chain is represented by r^i connected polymer blocks, numbered $s=1,2,\ldots, r^i$. The index i is adopted to denote the type of the molecule. An additional index j is used in order to account for the polydispersity. Thus, chains appear with several sizes, r^i_j, where j varies from minimum to a maximum value. In order to specify the segment conformation inside the block, we use the symbol sc, $\mathrm{sc}=1,2,\ldots, \mathrm{num_{sc}}$, where $\mathrm{num_{sc}}$ is the number of the possible configurations inside the block. One or more sc conformations may belong to same segment group (sg) of conformations $\mathrm{sg}=I$ or L (the V conformations are contained in the L group). In Scheme 1 we present the possible conformations inside a polymer block.

As shown in Scheme 1 the polymer-chain representation is done in three-dimensional (3D) space. Hence, the realization of the L conformation, corresponds to eight equivalent polymer blocks, which are achieved by rotation of two L-shaped block around the z-axis (see Scheme 1). In this way, although the volume fraction depends only on z, we can also estimate the polymer distribution and orientation in the other two axes.

Each block chain can assume a large number of possible conformations on the lattice. The conformation (c) is defined by specifying the layer numbers in which each of the successive block s finds itself (i.e. $c\equiv\{(s=1,\ z=z_1),\ (s=2,\ z=z_2),\ldots,(s=r^i_j,\ z=z_{r^i_j})\}$). The number of block chains (i,j) in conformation c is indicated as $n^c_{(i,j)}$. The block chains are distributed over the various possible configurations (sets of conformations $\{n^c_{(i,j)}\}$) in the lattice with statistical weights depending on the energy and entropy of each configuration. The proper description of the system will be given in the context of statistical physics by means of the grand canonical partition function. The partition function is a sum of terms,

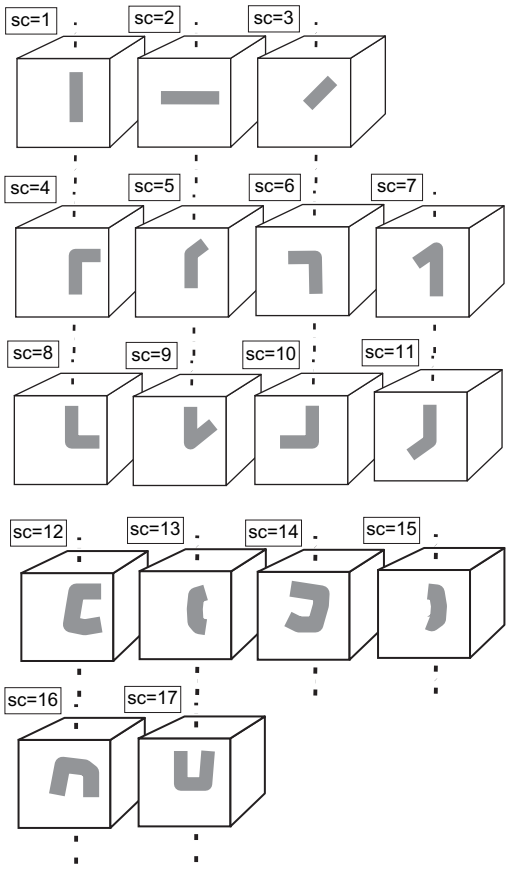

Scheme 1. The 17 possible polymer-segment conformations (sc) inside a cube block. Each block is characterized by the side of the cube on which the ends of the segment are put. We assume that the segment passes from the center of the cube. When rotating a block around the vertical axis (counterclockwise) we generate the next segment conformation. The V conformations start and end at same side of the cube. The conformations $\mathrm{sc}=1-3$ belong to the same segment group and have $\mathrm{sg}=I$. All the other segment conformations have $\mathrm{sg}=L$.

each related to a specific configuration of the block chain that fills the lattice.

The counting of ways of arranging block chains over available sites is readily performed in a lattice model. Equilibrium is the state at which they are distributed over the various possible conformations in the lattice such that the free energy (derived from the partition function) is at its minimum. We make the assumption of replacing the sum of several terms in the partition function by its maximum term (i.e. zero fluctuations of the density in the (x,y) directions). In order to obtain an expression for the number of molecules $n^c_{(i,j)}$ of chain type i of size r^i_j in conformation c, we minimize the natural logarithm of the maximum term of the partition function with respect to $n^c_{(i,j)}$, subject to the full occupancy constraint applied layerwise. We obtain the following expression [28]:

$$\ln\left(\frac{n^c_{(i,j)}}{L}\right) = \ln\left(\frac{\lambda^c}{r^{i^c}_j}\right) - 1 - \sum_{z=1}^{M} r^{i^c}_j(z)a(z) + \frac{\mu_i - \mu^*_i}{k_B T} - \frac{1}{k_B T}\frac{\partial(U-U^*)}{\partial n^c_{(i,j)}} \quad (1)$$

This expression for $n^c_{(i,j)}$ consists of an entropic term involving the connectivity factor λ^c; a hard-core repulsion through the Lagrance multipliers $a(z)$; the chemical potentials μ_i and μ^*_i of component i for homogeneous phases in equilibrium with the inhomogeneous and reference states, respectively; and the interaction and conformation energies of the chains relative to the reference state, $U - U^*$.

Although there are no restrictions for the angle formed between two successive blocks, there are prohibitions which deal with the polymer-chain continuity. When no continuity is succeeded in a pair of successive blocks, the energy of the equivalent bond of the block chain is infinity (for example, blocks $sc = 1$ and 2 have infinity energy no matter how we connect these blocks). The polymer-chain growth is accomplished by the success of different segment conformations and is done in continuous space. If the success of two blocks allows the continuity of the polymer chain, the bond energy of the block chain describes contributions from the torsion, bending and bond potential energies of the polymer segment. So in each block many different segment conformations occur. In order to avoid the introduction of many different bond energies, we match all the segment conformations with one of the I and L group of conformations. In this way although the formed angles are not limited by the lattice (0°, 90° and 180°), they are described by only two segment weighting factors (two independent variables). Each segment conformation is contained inside the lattice site and passes from the center of the cube block. It is produced by a certain number of monomers. We mention that the segment of the next block must start at the point where the segment of previous block finishes. So the bond energy depends on λ_i too. To each bond energy (ε_b) we associate the corresponding Boltzmann factor $\tau_b = \exp(-\varepsilon_b/k_B T)$. In Table 1 we present the possible bond energies. As was mentioned in our previous publication [30] it depends on the characteristic ratio (C_∞). The conformational energy is described as

$$\frac{U_S - U^*_S}{k_B T} = \sum_i \sum_c n^c_{(i,j)} \sum_{s=1}^{r^i_j} \frac{\varepsilon_{s;i;c} - \varepsilon^*_{i,s}}{k_B T}. \quad (2)$$

It is reasonable to assume that the various polymer conformations occupy different volume in the lattice site. Hence in cases where we have great variations from the average volume, the L conformation, which is also encaged in the same lattice site and includes higher energy, is assumed to have bigger volume. Obviously, we consider that an undisturbed polymer (random walk) has these segments in such a percentage (1/6 I conformation) that the average polymer density is as those measured experimentally.

Depending on the concentration of the polymer in the solution, the chain conformation may change. The interaction between polymer segments and solvent segments is calculated by the parameter χ, according to the mean field approach, using the ideas of the Flory–Huggins theory. In the context of this theory, the interaction energy between each pair of different species is given by the product of the volume fraction of each species multiplied with a parameter characteristic of the interaction. In our case, the solution consists of only one pair of two deferent chemical species. These are a homopolymer and a solvent symbolized as A and B, respectively. However, the involving interactions are more than one and in different levels (block-chain and polymer-chain interactions). In order to avoid the introduction of many parameters, we have exploited a new approach in which all interactions are derived from the basic one between polymer and solvent. We use the symbol $\phi^b_{AI}(\phi^b_{AL})$ for the volume fraction of the block containing the I (L) segment conformation and the symbol $\phi^{in}_{AI}(\phi^{in}_{AL})$ for the volume fraction of the polymer inside the block (or internal volume fraction). The volume fraction of the solvent inside the I block (L block) is $\phi^{in}_{BI}(\phi^{in}_{BL})$. The total volume fraction of the polymer in the solution is symbolized as ϕ_A and is the sum of the polymer in I and L conformations (ϕ_{AI} and ϕ_{AL}, respectively). Moreover the volume fraction of the solvent block is ϕ^b_B and the total volume fraction of the solvent is ϕ_B. Then the interaction energy is described as

$$\frac{U_F - U^*_F}{k_B T} = \frac{1}{2}\left[L\sum_{z=1}^{M}\phi_A(z)\chi_{AB}\langle\phi_B(z)\rangle - \sum_i n_{(i,j)} r^i_j \phi^*_{Ai}\chi_{AB}\phi^*_{Bi}\right] \quad (3)$$

where ϕ^*_{Ai} and ϕ^*_{Bi} are the volume fractions in the reference state.

If we set the interaction (and conformational) energy to zero in the reference state, then Eq. (3) for the inhomogeneous state at z layer for sites filled with polymer and solvent can be rewritten as

Table 1
The non-zero Boltzmann factors

sc = 1	sc = 2	sc = 3	sc = 4	sc = 5	sc = 6	sc = 7
$\tau_{1,0,-1}=\tau_I$	$\tau_{2,2,0}=\tau_I^{**}$	$\tau_{3,3,0}=\tau_I^{**}$	$\tau_{4,0,-1}=\tau_L$	$\tau_{5,0,-1}=\tau_L$	$\tau_{6,0,-1}=\tau_L$	$\tau_{7,0,-1}=\tau_L$
$\tau_{1,1,-1}=\tau_I$	$\tau_{2,4,0}=\tau_I^{*}$	$\tau_{3,5,0}=\tau_I^{*}$	$\tau_{4,1,-1}=\tau_L$	$\tau_{5,1,-1}=\tau_L$	$\tau_{6,1,-1}=\tau_L$	$\tau_{7,1,-1}=\tau_L$
$\tau_{1,1,+1}=\tau_I$	$\tau_{2,6,0}=\tau_I^{*}$	$\tau_{3,7,0}=\tau_I^{*}$	$\tau_{4,2,0}=\tau_L^{*}$	$\tau_{5,3,0}=\tau_L^{*}$	$\tau_{6,2,0}=\tau_L^{*}$	$\tau_{7,3,0}=\tau_L^{*}$
$\tau_{1,4,+1}=\tau_I$	$\tau_{2,8,0}=\tau_I^{*}$	$\tau_{3,9,0}=\tau_I^{*}$	$\tau_{4,6,0}=\tau_L^{*}$	$\tau_{5,7,0}=\tau_L^{*}$	$\tau_{6,4,0}=\tau_L^{*}$	$\tau_{7,5,0}=\tau_L^{*}$
$\tau_{1,5,+1}=\tau_I$	$\tau_{2,10,0}=\tau_I^{*}$	$\tau_{3,11,0}=\tau_I^{*}$	$\tau_{4,8,-1}=\tau_L$	$\tau_{5,8,-1}=\tau_L$	$\tau_{6,8,-1}=\tau_L$	$\tau_{7,8,-1}=\tau_L$
$\tau_{1,6,+1}=\tau_I$	$\tau_{2,12,0}=\tau_I^{*}$	$\tau_{3,13,0}=\tau_I^{*}$	$\tau_{4,9,-1}=\tau_L$	$\tau_{5,9,-1}=\tau_L$	$\tau_{6,8,0}=\tau_L^{*}$	$\tau_{7,9,-1}=\tau_L$
$\tau_{1,7,+1}=\tau_I$	$\tau_{2,14,0}=\tau_I^{*}$	$\tau_{3,15,0}=\tau_I^{*}$	$\tau_{4,10,-1}=\tau_L$	$\tau_{5,10,-1}=\tau_L$	$\tau_{6,9,-1}=\tau_L$	$\tau_{7,9,0}=\tau_L^{*}$
$\tau_{1,8,-1}=\tau_I$			$\tau_{4,10,0}=\tau_L^{*}$	$\tau_{5,11,-1}=\tau_L$	$\tau_{6,10,-1}=\tau_L$	$\tau_{7,10,-1}=\tau_L$
$\tau_{1,9,-1}=\tau_I$			$\tau_{4,11,-1}=\tau_L$	$\tau_{5,11,0}=\tau_L^{*}$	$\tau_{6,11,-1}=\tau_L$	$\tau_{7,11,-1}=\tau_L$
$\tau_{1,10,-1}=\tau_I$			$\tau_{4,14,0}=\tau_L^{*}$	$\tau_{5,15,0}=\tau_L^{*}$	$\tau_{6,12,0}=\tau_L^{*}$	$\tau_{7,13,0}=\tau_L^{*}$
$\tau_{1,11,-1}=\tau_I$			$\tau_{4,16,-1}=\tau_L$	$\tau_{5,16,-1}=\tau_L$	$\tau_{6,16,-1}=\tau_L$	$\tau_{7,16,-1}=\tau_L$
$\tau_{1,16,-1}=\tau_I$						
$\tau_{1,17,+1}=\tau_I$						

sc = 8	sc = 9	sc = 10	sc = 11	sc = 12	sc = 13	sc = 14
$\tau_{8,1,+1}=\tau_L$	$\tau_{9,1,+1}=\tau_L$	$\tau_{10,1,+1}=\tau_L$	$\tau_{11,1,+1}=\tau_L$	$\tau_{12,2,0}=\tau_L^{*}$	$\tau_{13,3,0}=\tau_L^{*}$	$\tau_{14,2,0}=\tau_L^{*}$
$\tau_{8,2,0}=\tau_L^{*}$	$\tau_{9,3,0}=\tau_L^{*}$	$\tau_{10,2,0}=\tau_L^{*}$	$\tau_{11,3,0}=\tau_L^{*}$	$\tau_{12,6,0}=\tau_L^{*}$	$\tau_{13,7,0}=\tau_L^{*}$	$\tau_{14,4,0}=\tau_L^{*}$
$\tau_{8,4,+1}=\tau_L$	$\tau_{9,4,+1}=\tau_L$	$\tau_{10,4,0}=\tau_L^{*}$	$\tau_{11,4,+1}=\tau_L$	$\tau_{12,10,0}=\tau_L^{*}$	$\tau_{13,11,0}=\tau_L^{*}$	$\tau_{14,8,0}=\tau_L^{*}$
$\tau_{8,5,+1}=\tau_L$	$\tau_{9,5,+1}=\tau_L$	$\tau_{10,4,+1}=\tau_L$	$\tau_{11,5,0}=\tau_L^{*}$	$\tau_{12,14,0}=\tau_L^{*}$	$\tau_{13,15,0}=\tau_L^{*}$	$\tau_{14,12,0}=\tau_L^{*}$
$\tau_{8,6,0}=\tau_L^{*}$	$\tau_{9,6,+1}=\tau_L$	$\tau_{10,5,+1}=\tau_L$	$\tau_{11,5,+1}=\tau_L$			
$\tau_{8,6,+1}=\tau_L$	$\tau_{9,7,0}=\tau_L^{*}$	$\tau_{10,6,+1}=\tau_L$	$\tau_{11,6,+1}=\tau_L$			
$\tau_{8,7,+1}=\tau_L$	$\tau_{9,7,+1}=\tau_L$	$\tau_{10,7,+1}=\tau_L$	$\tau_{11,7,+1}=\tau_L$			
$\tau_{8,10,0}=\tau_L^{*}$	$\tau_{9,11,0}=\tau_L^{*}$	$\tau_{10,8,0}=\tau_L^{*}$	$\tau_{11,9,0}=\tau_L^{*}$			
$\tau_{8,14,0}=\tau_L^{*}$	$\tau_{9,15,0}=\tau_L^{*}$	$\tau_{10,12,0}=\tau_L^{*}$	$\tau_{11,13,0}=\tau_L^{*}$			
$\tau_{8,17,+1}=\tau_L$	$\tau_{9,17,+1}=\tau_L$	$\tau_{10,17,+1}=\tau_L$	$\tau_{11,17,+1}=\tau_L$			

sc = 15	sc = 16	sc = 17
$\tau_{15,3,0}=\tau_L^{*}$	$\tau_{16,1,+1}=\tau_L$	$\tau_{17,1,-1}=\tau_L$
$\tau_{15,5,0}=\tau_L^{*}$	$\tau_{16,4,+1}=\tau_L$	$\tau_{17,8,-1}=\tau_L$
$\tau_{15,9,0}=\tau_L^{*}$	$\tau_{16,5,+1}=\tau_L$	$\tau_{17,9,-1}=\tau_L$
$\tau_{15,13,0}=\tau_L^{*}$	$\tau_{16,6,+1}=\tau_L$	$\tau_{17,10,-1}=\tau_L$
	$\tau_{16,7,+1}=\tau_L$	$\tau_{17,11,-1}=\tau_L$
	$\tau_{16,17,+1}=\tau_L$	$\tau_{17,16,-1}=\tau_L$

For the surface we give the index 0. The chain can start with the first, fourth, fifth, sixth and seventh blocks. The factors τ_{sg}^{*} and τ_{sg}^{**} take different values depending on the kind of the chain walk (random or disturbed). When the growth follows the random walk: $\tau_I^{**}=(2/4)\tau_I$, $\tau_I^{*}=(1/4)\tau_I$, $\tau_L^{*}=(1/4)\tau_L$. While in the disturbed walk: $\tau_I^{**}=\delta(2/4)\tau_I$, $\tau_I^{*}=\delta(1/4)\tau_I$, $\tau_L^{*}=\delta(1/4)\tau_L$ ($\delta>1$). The solvent ($\mathrm{num_{sc}}+1$) can follow after every block and from every side of the cube (every λ_i). The obtained bond energy for this case is τ_{sg}.

$$\begin{aligned}\frac{L}{2}\phi_{\mathrm{A}}(z)\chi_{\mathrm{AB}}\langle\phi_{\mathrm{B}}(z)\rangle &= \frac{L}{2}\phi_{\mathrm{A}I}(z)\chi_{\mathrm{AB}}\langle\phi_{\mathrm{B}}(z)\rangle+\frac{L}{2}\phi_{\mathrm{A}L}(z)\chi_{\mathrm{AB}}\langle\phi_{\mathrm{B}}(z)\rangle\\ &= \frac{L}{2}\phi^{\mathrm{b}}_{\mathrm{A}I}(z)\phi^{\mathrm{in}}_{\mathrm{A}I}\chi_{\mathrm{AB}}\left\langle\phi^{\mathrm{b}}_{\mathrm{B}}(z)+\phi^{\mathrm{in}}_{\mathrm{B}I}\phi^{\mathrm{b}}_{\mathrm{A}I}(z)+\phi^{\mathrm{in}}_{\mathrm{B}L}\phi^{\mathrm{b}}_{\mathrm{A}L}(z)\right\rangle+\frac{L}{2}\phi^{\mathrm{b}}_{\mathrm{A}L}(z)\phi^{\mathrm{in}}_{\mathrm{A}L}\chi_{\mathrm{AB}}\left\langle\phi^{\mathrm{b}}_{\mathrm{B}}(z)+\phi^{\mathrm{in}}_{\mathrm{B}L}\phi^{\mathrm{b}}_{\mathrm{A}L}(z)+\phi^{\mathrm{in}}_{\mathrm{B}I}\phi^{\mathrm{b}}_{\mathrm{A}I}(z)\right\rangle\\ &= \frac{L}{2}\phi^{\mathrm{b}}_{\mathrm{A}I}(z)\,\phi^{\mathrm{in}}_{\mathrm{A}I}\chi_{\mathrm{AB}}\left\langle\phi^{\mathrm{b}}_{\mathrm{B}}(z)\right\rangle+\frac{L}{2}\phi^{\mathrm{b}}_{\mathrm{A}I}(z)\,\phi^{\mathrm{in}}_{\mathrm{A}I}\chi_{\mathrm{AB}}\phi^{\mathrm{in}}_{\mathrm{B}I}\left\langle\phi^{\mathrm{b}}_{\mathrm{A}I}(z)\right\rangle+\frac{L}{2}\phi^{\mathrm{b}}_{\mathrm{A}I}(z)\,\phi^{\mathrm{in}}_{\mathrm{A}I}\chi_{\mathrm{AB}}\phi^{\mathrm{in}}_{\mathrm{B}L}\left\langle\phi^{\mathrm{b}}_{\mathrm{A}L}(z)\right\rangle\\ &\quad+\frac{L}{2}\phi^{\mathrm{b}}_{\mathrm{A}L}(z)\,\phi^{\mathrm{in}}_{\mathrm{A}L}\chi_{\mathrm{AB}}\left\langle\phi^{\mathrm{b}}_{\mathrm{B}}(z)\right\rangle+\frac{L}{2}\phi^{\mathrm{b}}_{\mathrm{A}L}(z)\,\phi^{\mathrm{in}}_{\mathrm{A}L}\chi_{\mathrm{AB}}\phi^{\mathrm{in}}_{\mathrm{B}L}\left\langle\phi^{\mathrm{b}}_{\mathrm{A}L}(z)\right\rangle+\frac{L}{2}\phi^{\mathrm{b}}_{\mathrm{A}L}(z)\,\phi^{\mathrm{in}}_{\mathrm{A}L}\chi_{\mathrm{AB}}\phi^{\mathrm{in}}_{\mathrm{B}I}\left\langle\phi^{\mathrm{b}}_{\mathrm{A}I}(z)\right\rangle\end{aligned}\tag{4}$$

The quantities between the z-dependent volume fractions are the corresponding χ parameters for the involving lattice interactions. More details are given in Section 2.3.

The system can be described in a mean field self-consistent approximation in terms of a segment potential $u_{\mathrm{b}}(z)$ depending only on the kind of the segment (b = AI, AL and B here). In our case we have three different blocks. The two polymer blocks (I and L) and the solvent block. Generally, it stands

$$u_{\mathrm{b}}(z)=kT\alpha(z)+\frac{\partial U/L}{\partial\phi_{\mathrm{b}}(z)}+u_{\mathrm{b}}^{\mathrm{ref}}\tag{5}$$

We introduce the segment weighting factor, $G(z)\equiv \mathrm{e}^{-u_{\mathrm{b}}(z)/kT}$. The weight $G(z)$ is proportional to the probability of finding a segment in layer z of the interfacial system, relative to finding it in the bulk. Then the statistical weight for finding an end of an s-segment long chain in layer z, $G(z;s)$, is defined. We can find a recursion relation, which is solved once we know a proper initial condition. For the forward propagation the recursion relation has the following expression ($s>1$):

$$G\big(z,s_{\mathrm{sc}}\big|1\big)=G\big(z,s_{\mathrm{sg}}\big)\langle G(z,s-1|1)\rangle\tag{6}$$

where $\langle G(z,s-1|1)\rangle$

$$\equiv \sum_{s_{sc}=1}^{num_{sc}} \sum_{(s-1)_{sc}=1}^{num_{sc}} \sum_{i=-1}^{+1} \lambda_i \tau_{s_{sc},(s-1)_{sc},i} G\big(z+i,(s-1)_{sc}\big|1\big) \quad (6')$$

For the backward propagation ($s<r$):

$$G\big(z,s_{sc}\big|r\big) = G\big(z,s_{sg}\big)\langle G(z,s-1|r)\rangle \quad (7)$$

where $\langle G(z,s-1|r)\rangle$

$$\equiv \sum_{s_{sc}=1}^{num_{sc}} \sum_{(s-1)_{sc}=1}^{num_{sc}} \sum_{i=-1}^{+1} \lambda_i \tau_{s_{sc},(s-1)_{sc},i} G\big(z+i,(s-1)_{sc}\big|r\big) \quad (7')$$

All segment conformations characterized as I have the segment weighting factor $G(z,s_I)$ and the volume fraction ϕ^b_{AI}. Also all L and V conformations have the weighting factor $G(z,s_L)$ and the volume fraction ϕ^b_{AL}.

When $s=1$ or $s=r$ then $(s-1)_{sc}$ can either take the value 0 in order to describe the surface (forward propagation) or the value $(num_{sc}+1)$ for the solvent after the last polymer segment (backward propagation). Of course for the grafted chains $G(z,1_{sg}/1)=G(z,1_{sg})\delta_{z,1}$. For the solvent case, we only use the weight $G(z)$.

Then by means of a composition law we find the volume fractions. For the grafted chains:

$$\phi(z) = \sum_{k=1}^{r^{max}} \sum_{s=1}^{k} \sum_{s_{sc}=1}^{num_{sc}} \phi^{in}_{A_{sg}} \times \big\{G\big(z,s_{sg}\big)^{-1}\tau_{sg}(C_k G(z,s_{sc}|1)G(z,s_{sc}|k))\big\} \quad (8)$$

where the factor $G(z,s_{sg})^{-1}\tau_{sg}^{-1}$ is set in order to take care of the double counting.

By properly rearranging the order of the summation we get

$$\phi(z) = \sum_{s=1}^{r^{max}} \sum_{s_{sc}=1}^{num_{sc}} \phi^{in}_{A_{sg}} \big\{G\big(z,s_{sg}\big)^{-1}\tau_{sg}(G(z,s_{sc}|1)[C_s G(z,s_{sc}|s) + G(z,s_{sc}/\{k\geq s+1\})])\big\} \quad (9)$$

$$\text{where } C_s = \sigma\frac{n_s}{n_{total}}\frac{1}{\sum_z G(z,s/1)} \quad (10)$$

and σ is the surface density.

The solvent's volume fraction is

$$\phi(z) = C_1 G(z) \quad (11)$$

$$\text{where } C_1 = \frac{M-\overline{r}\sigma}{\sum_z G(z)} \quad (12)$$

M is the number of the layers.

2.2. Brush regime: disturbed walk

The polymer-chain growth in a brush is restricted by the presence of the other chains due to high polymer concentration. In the brush case, we have a definite deviation from the random walk. The chain growth has been compared to the movement of a charged particle in a force field [3]. In the brush regime, it is expected an increase of the possibilities to move perpendicular to the substrate. Hence in the present work, our objective is to give a different (larger) weight to the more uniformly stretched conformations that are likely to happen in this region.

When two cube blocks lie in the same layer, there are 16 ways to stand side by side. For the cases where a pair of blocks can allow the chain continuity e.g. the blocks with $sc=4$ and 2, only one placement can permit the polymer-chain development. The block with $sc=4$ is surrounded by $(4/6)\phi^b_{A_{sc=2}}$ blocks that lie in the same layer. Because of the 3-D representation of the polymer-segment conformation, only $(1/6)\phi^b_{A_{sc=2}}$ are useful for the polymer growth. So in order to describe the random walk, the Boltzmann factor must get the value $(1/4)\tau_b$, if $\lambda_i=\lambda_0$. In this way we have $\lambda_0(1/4)\tau_b\phi^b_{A_{sc}} = (1/6)\tau_b\phi^b_{A_{sc}}$. The introduction of the polymer preference to stretch uniformly perpendicular to surface is done by multiplying the Boltzmann factor for all the possible block bonds parallel to the surface we another factor δ. In our example, instead of having $\tau_{4,2,0}=(1/4)\tau_L$, we set $\tau_{4,2,0}=\delta(1/4)\tau_L$. The parameter δ is a measure of the deviation of the random walk and has no units. When $\delta=1$ we have a random walk development.

The product of all λ_i gives the number of possible configurations of the block chain on the lattice divided with the configurations in bulk (Z^{r-1} number of configurations). Let us assume that the Boltzmann factor (τ_b) is constant for both versions of chain development. This means that for disturbed walk stands: $\lambda_0\delta(1/4)\times\tau_b\phi^b_{A_{sc}}$, while for random walk: $\lambda_0(1/4)\times\tau_b\phi^b_{A_{sc}}$. As mentioned before, the 3-D representation on a cube lattice is described by six different λ_i. Each λ_i has the value 1/6. When the polymer chooses to "move" parallel to the surface in the disturbed walk stands: $\lambda'_0 = \lambda_0\delta(1/4) = (\delta/6)$; while in the random walk stands: $\lambda'_0 = \lambda_0(1/4) = (1/6)$, describing that the previous block is in contact with only the one side of the cube lattice site. So in the disturbed walk one step parallel to the surface is equivalent to $(\delta/6)\times 6=\delta$ combinations of polymer (imaginary) placement, while in random walk describes only one (real) placement. As a result the chain can "pay" easier the entropic cost and this favor the configuration perpendicular to the surface. If chains do not have the entropic benefit, they have to take conformations that distribute them unevenly parallel to the surface. Those flatten configurations are obtained when the chains take a mushroom shape (Scheme 2a). The reason is that chains that try to flatten on the first layer have to take the shape of a worm (loops parallel to the surface and trains developed along the surface). Because of the surface obstacle, the polymer cannot develop freely and usually such conformations require an adsorptive surface [6]. As a result, they stretch at the first one or two layers and then they distribute parallel to the surface. But at high concentrations such configurations are unlike to happen. In the brush case, where $\langle R^2\rangle^{1/2} \gg \sqrt{1/\pi\sigma}$, the polymer conformation is mainly determined by the enthalpic factor. So it is more possible for the chains to take

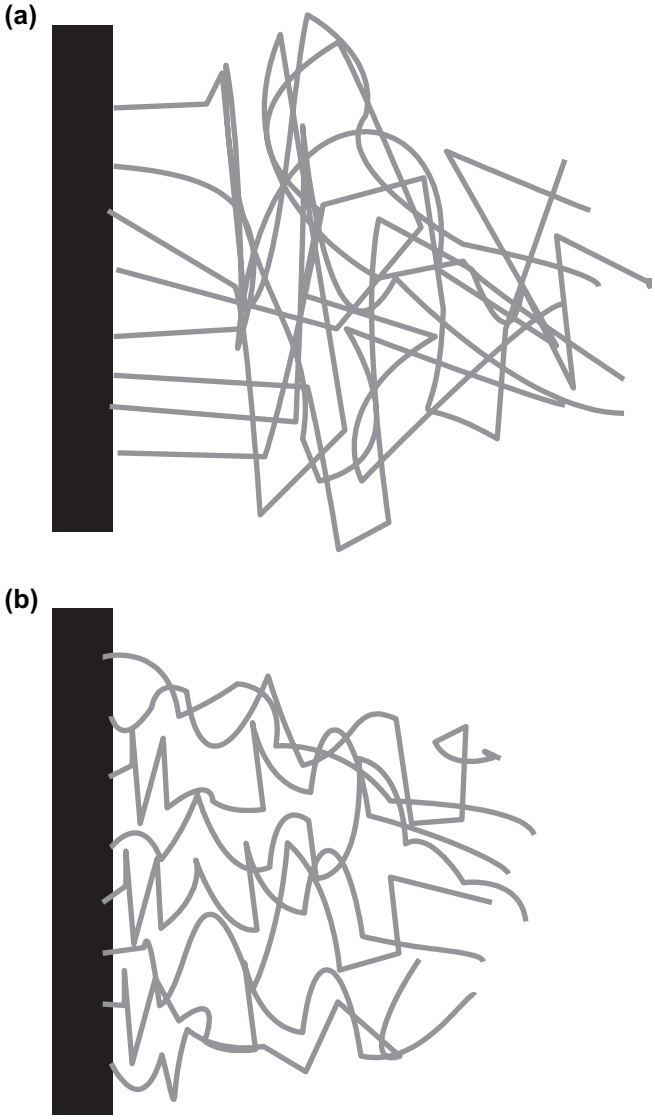

Scheme 2. Schematic representation of the polymer brush for the cases of (a) random walk (mushroom-like conformations) and (b) disturbed walk (brush-like conformations) growth. The appearance of the depletion layer in the case of random walk is attributed to the tendency of the chain to reduce the free energy by distributing its main part in the first layers after the first one (mushroom shape). This behavior is mainly guided by the entropic factor. By giving more weight to more uniformly stretched distributions perpendicular to the surface we obtain more brush-like configurations as we observe the disappearance of the depletion layer.

uniformly stretched configurations that are shown in Scheme 2b. As the more flattened conformations are reduced, their place is taken by more realistic brush conformations.

Conclusively in the random walk growth, chains that take conformations like in Schemes 2a and 3a would be very stable (as more stretched conformations also contribute to the total polymer volume fraction in smaller proportion). The reduction of contacts between polymer and solvent in high concentrations is done by squeezing only the flatten part of the mushroom-like chain. The ''stem'' of the mushroom configurations is already too elongated. As a result, we get overestimated extension of the brush height. In the same case,

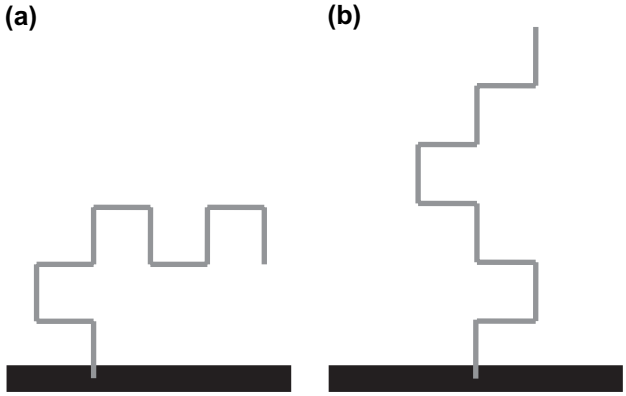

Scheme 3. Characteristic types of chain conformations on a cube lattice. The position of each segment depends only on the distance from the surface (z). So the existence of one segment parallel to the surface represents all the possible placements in this parallel level. (a) Flatten conformations, distributing the polymer parallel to the surface. (b) Stretched conformations, with more uniform distribution in the z-axis.

conformations like in Schemes 2b and 3b would have much less enthalpic cost but this could not compensate the entropic reduction. So in the random walk case the conformation depicted in Scheme 3a is very preferable in a wide range of concentrations. On the other hand in the disturbed walk the flatten configurations that resemble Scheme 3a obtain high volume fraction, that is substantially the total polymer volume fraction ($\lambda_0' = \delta/6$). So at high concentrations these configurations are very unfavorable. In the same time, the conformations like the one in Scheme 3b distribute the chains in more layers and have an enthalpic advantage. As in the disturbed walk the chains are represented substantially by one type of conformations (3a or 3b), at high concentrations they prefer the 3b type. When surface density reduces the disturbed walk causes the chains to flatten in first layers and shrink intensely. That is why at low surface densities (low concentrations) we prefer to describe the chain's growth using the random walk. Besides in low concentrations there is enough space for the random walk growth. The version of the new model using the random walk ($\delta = 1$) is called (rw) bnSCF and gives more weight to conformations that resemble a mushroom (Schemes 2a and 3a). In Table 1 we present Boltzmann factors for both versions.

2.3. Phase separation, χ_c

The determination of the critical value for the interaction parameter, where phase separation occurs, is done using the Flory–Huggins theory. In our model, the interactions occur between the polymer segment and the solvent, which surrounds it inside each block (internal energy) but also between polymer blocks and solvent blocks.

Let us assume the existence of a second traditional lattice (Flory–Huggins theory) on which we put only polymer segments and solvent segments of the same volume. Then each segment interacts with another solvent molecule with the interaction parameter χ_{AB}. We can estimate the interaction

parameters on the block lattice by counting the number of contacts on a traditional lattice. If the average polymer volume fraction inside the block is $\overline{\phi}_{\mathrm{A}}^{\mathrm{in}}$ then each polymer block interacts with another solvent block with an interaction parameter $\overline{\phi}_{\mathrm{A}}^{\mathrm{in}}\chi_{\mathrm{AB}}$, since the total number of contacts between polymer and solvent in the two blocks is counted $\overline{\phi}_{\mathrm{A}}^{\mathrm{in}}\cdot 1$. Moreover each polymer segment interacts with the surrounding solvent molecules in every polymer block with an interaction parameter $\overline{\phi}_{\mathrm{A}}^{\mathrm{in}}\chi_{\mathrm{AB}}\overline{\phi}_{\mathrm{B}}^{\mathrm{in}}$.

We note that in equilibrium the true volume fraction of the polymer ($\phi_{\mathrm{A}}^{\mathrm{b}}\overline{\phi}_{\mathrm{A}}^{\mathrm{in}}$) is considered. Nevertheless $\overline{\phi}_{\mathrm{A}}^{\mathrm{in}}$ sets a limit in the higher value of the polymer volume fraction inside the solution. In most cases of good solution (including the ones studied in this work) this is a satisfactory limit as the total polymer volume fraction does not exceed the $\overline{\phi}_{\mathrm{A}}^{\mathrm{in}}$. The reason is that the maximum is defined such as a well-diluted segment would be in *I* conformation and fully surrounded by solvent molecules (for the internal volume fraction of *L* conformation see Section 2.4, Eq. (26)). If the volume of a monomer is α_{p}^3 and the volume of a solvent molecule is α_{s}^3, then the cube that contains the segment and the appropriate number of solvent molecules has length approximately $l\approx\sqrt{4\alpha_{\mathrm{p}}\alpha_{\mathrm{s}}+\alpha_{\mathrm{p}}^2}$. This is usually higher than the Flory-segment length [28,29] and close to the Kuhn segment. Instead of determining the lattice site size as another parameter we defined it from the Kuhn segment. For cases that a higher maximum in the internal volume fraction is needed, these are situations where segments being very close have important statistical weight, we just have to put more segments in the same block. If for example two segments are together then the internal volume fraction is double and the interaction parameter is equal to $\overline{2\phi}_{\mathrm{A}}^{\mathrm{in}}\chi_{\mathrm{AB}}$. This consequence of the variable mean field is reasonable since cases of crowded blocks correspond to situations of worse solvency.

The Gibbs free energy for a polymer chain showing no density fluctuations is given by the following equation [32]:

$$\frac{\Delta G_{\mathrm{mix}}}{RTN}=\phi_{\mathrm{B}}^{\mathrm{b}}\ln\phi_{\mathrm{B}}^{\mathrm{b}}+\frac{\phi_{\mathrm{A}}^{\mathrm{b}}}{x}\ln\phi_{\mathrm{A}}^{\mathrm{b}}+\phi_{\mathrm{A}}^{\mathrm{b}}\overline{\phi}_{\mathrm{A}}^{\mathrm{in}}\chi_{\mathrm{AB}}\phi_{\mathrm{B}}^{\mathrm{b}}+\phi_{\mathrm{A}}^{\mathrm{b}}\overline{\phi}_{\mathrm{A}}^{\mathrm{in}}\chi_{\mathrm{AB}}\overline{\phi}_{\mathrm{B}}^{\mathrm{in}}\phi_{\mathrm{A}}^{\mathrm{b}} \tag{13}$$

N is the total number blocks (solvent and polymer), *x* is the degree of polymerization and $R=k_{\mathrm{B}}N_{\mathrm{A}}$ (N_{A} is the Avogadro's number).

Then the chemical potential is obtained as

$$\frac{\mu_{\mathrm{B}}-\mu_{\mathrm{B}}^{*}}{RT}=\frac{\Delta G_{\mathrm{mix}}}{RTN}+\phi_{\mathrm{A}}^{\mathrm{b}}\frac{\mathrm{d}(\Delta G_{\mathrm{mix}}/RTN)}{\mathrm{d}\phi_{\mathrm{B}}^{\mathrm{b}}} \tag{14}$$

We calculate the critical value (χ_{c}) of the interaction parameter by solving the following system of two equations:

$$\frac{\mathrm{d}\mu_{\mathrm{B}}}{\mathrm{d}\phi_{\mathrm{B}}^{\mathrm{b}}}=0,\ \frac{\mathrm{d}^2\mu_{\mathrm{B}}}{\mathrm{d}\phi_{\mathrm{B}}^{\mathrm{b}^2}}=0 \tag{15}$$

The critical value is given as $\chi_{\mathrm{c}}=\dfrac{1}{2\left(\overline{\phi}_{\mathrm{A}}^{\mathrm{in}}-\overline{\phi}_{\mathrm{A}}^{\mathrm{in}}\overline{\phi}_{\mathrm{B}}^{\mathrm{in}}\right)}$ (16)

If the polymer block is only filled with polymer then $\overline{\phi}_{\mathrm{A}}^{\mathrm{in}}=1$ and $\overline{\phi}_{\mathrm{B}}^{\mathrm{in}}=0$. In this case $\chi_{\mathrm{c}}=0.5$ and the bnSCF collapses to the traditional nSCF.

If we call χ^{b} the interaction parameter in our bnSCF method, then the relation with the corresponding parameter χ^{FH} in the traditional nSCF is

$$\chi^{\mathrm{FH}}=0.5\frac{\chi^{\mathrm{b}}}{\chi_{\mathrm{c}}}. \tag{17}$$

The χ_{c} obtained by this approach is usually higher than the one achieved introducing all the parameters listed below. Hence, the corresponding χ^{FH} may have a little higher value. This is owed to the introduction of the polymer stiffness and the segment density fluctuation. Also the preference to move perpendicular to the surface causes chain to be more sensitive in the χ changes. An analogue deviation occur in the nSCF where polymer stiffness influences the entropic change (less conformations are possible in the inhomogeneous phase).

2.4. Mapping real polymers onto the lattice

The lattice size (l) is given by the length of Kuhn segment (l_{K}) and so it is related to stiffness parameter C_∞ by the following expression:

$$l=l_{\mathrm{K}}=l_{\mathrm{b}}\frac{C_\infty}{\sin\left(\frac{\theta_{\mathrm{b}}}{2}\right)} \tag{18}$$

where the mean square end-to-end distance of the chain is given as

$$\left\langle R^2\right\rangle=C_\infty n_{\mathrm{b}}l_{\mathrm{b}}^2 \tag{19}$$

l_{b} is the bond length and θ_{b} is the bond angle along the chain backbone and n_{b} is the number of bonds.

The volume of the polymer segment inside the lattice site is calculated using the approach of the Flory segment, mentioned in previous work [28–30]. The Flory segment, of length l_{F}, is usually shorter than the Kuhn segment. It can be defined such that a chain will have the same maximally extended length (end-to-end distance in all-trans conformation) and volume in the Flory segment representation as are measured experimentally.

$$l_{\mathrm{F}}=\left[\frac{n_{\mathrm{m}}M_{\mathrm{m}}}{N_{\mathrm{A}}\rho n_{\mathrm{b}}l_{\mathrm{b}}\sin\left(\frac{\theta_{\mathrm{b}}}{2}\right)}\right]^{1/2} \tag{20}$$

where n_{m} is the degree of polymerization, M_{m} is the monomer molecular weight, ρ the mass density of the polymer and N_{A} is Avogadro's number, n_{b} is the number of chemical bonds per chain. According to this approximation, the average polymer volume fraction inside a lattice site is

$$\overline{\phi}_{\mathrm{A}}^{\mathrm{in}} = \frac{n_{\mathrm{m}} M_{\mathrm{m}}}{N_{\mathrm{A}} \rho n_{\mathrm{b}} l_{\mathrm{b}} \sin\left(\frac{\theta_{\mathrm{b}}}{2}\right)} \frac{1}{l^2} \tag{21}$$

The number of monomers per block (n_{mpb}) is given by the equation:

$$n_{\mathrm{mpb}} = n_{\mathrm{mpF}} \frac{l}{l_{\mathrm{f}}} \tag{22}$$

where n_{mpF} is the number of monomers per Flory segment

$$n_{\mathrm{mpF}} = \frac{N_{\mathrm{A}} \rho l_{\mathrm{F}}^3}{M_{\mathrm{m}}} \tag{23}$$

In the cases of big monomers (usually those that substitute the hydrogen with a bigger unit) there are no important variations from the average volume fraction ($\overline{\phi}_{\mathrm{A}}^{\mathrm{in}}$). Nevertheless rod-like monomers such as polyethylene may occupy much different space depending on the conformation they take. Also in cases of hydrophobic hydration in some areas of the solution, the polymer may obtain less volume conformations [34]. The part of the polymer that is surrounded by solvent molecules is stretched and so takes the *I* conformaion. Under these circumstances the volume of the *I* segment conformation is smaller than the *L* segment volume. The cross-section for the *I* conformation is usually set around the α_{p}^2,

$$\text{where } \alpha_{\mathrm{p}}^3 = \frac{M_{\mathrm{m}}}{N_{\mathrm{A}} \rho} \quad (\text{monomer's volume}). \tag{24}$$

A more accurate estimation depends on the polymer's geometry.

So the volume fraction of the *I* conformation is

$$\phi_{\mathrm{A}I}^{\mathrm{in}} = \frac{\alpha_{\mathrm{p}}^2 l}{l^3} \tag{25}$$

If we consider a random walk for an undisturbed polymer chain (the condition of the polymer when experimental data are collected) then

$$\overline{\phi}_{\mathrm{A}}^{\mathrm{in}} = \frac{\phi_{\mathrm{A}I}^{\mathrm{in}} + 5\phi_{\mathrm{A}L}^{\mathrm{in}}}{6} \Rightarrow \phi_{\mathrm{A}L}^{\mathrm{in}} = \frac{6\overline{\phi}_{\mathrm{A}}^{\mathrm{in}} - \phi_{\mathrm{A}I}^{\mathrm{in}}}{5}. \tag{26}$$

In most cases the Kuhn segment is almost twice the Flory segment. Therefore usually a block contains only one angle formed by almost two Flory segments [29,30]. The bond energies are determined from the characteristic ratios by matching the mean-square end-to-end distance between a real chain and a chain of correlated Flory segments. The characteristic ratio of the correlated Flory chain (C_∞^{F}) is

$$C_\infty^{\mathrm{F}} = \frac{C_\infty n_{\mathrm{b}} l_{\mathrm{b}}^2}{(r-1) l_{\mathrm{F}}^2} \tag{27}$$

in which C_∞^{F} is the characteristic ratio of the correlated Flory chain.

Assuming that back-folding (*V*) inside the block conformations is a special case of *L* conformation, the characteristic ratio of the Flory chain is related to the bond statistical weights by

$$C_\infty^{\mathrm{F}} = 1 + \frac{\tau_I}{2\tau_L} = 1 + \frac{1}{2} \mathrm{e}^{(\varepsilon_L - \varepsilon_I)/kT} \tag{28}$$

Since the characteristic ratio depends only on the difference between the energies ($\varepsilon_L - \varepsilon_I$), one of them (in our case ε_I) may be set arbitrarily to zero. So the bending energy ε_L can be estimated once the characteristic ratio C_∞ is known.

$$\tau_L = \frac{1}{2\left(C_\infty^{\mathrm{F}} - 1\right)} \tag{28'}$$

3. System studied

3.1. PP in a good solvent

Isotactic polypropylene is a very well-studied polymer. It was previously studied by nSCF method [29] for the case of a melt. Because the theoretical results were considered very satisfactory and we use them in order to check our new method. Only this time we take the PP as being solved by a good solvent.

It is known that the length of the C–C bond is 1.54 Å and the angle between two consecutive C–C bonds is 112°. In Ref. [31] we find expressions for the density as a function of the pressure and temperature. In the results we present here we have assumed that the temperature of our system is 220 °C, which is higher than the melting point [29,31].

For the nSCF the characteristic ratio (C_∞) is 5.7 [29]. For this C_∞, Eqs. (27) and (28) give a bending energy $\varepsilon_L = 0.40 k_{\mathrm{B}}T$. The Flory interaction parameter between the PP and the good solvent is $\chi = 0.1$. For PP, the Flory segment length from Eq. (20) is $l_{\mathrm{F}} = 6.06$ Å, and the number of chemical (propylene) monomers in a Flory segment is 2.37.

In the bnSCF the characteristic ratio (C_∞) is set 5.8. So the bending energy is (Eqs. (27) and (28)) $\varepsilon_L = 0.44 k_{\mathrm{B}}T$. The Kuhn statistical segment from Eq. (18) is $l_{\mathrm{K}} = 10.77$ Å. The number of monomers per block is 4.21. The interaction parameter between the PP and the good solvent is $\chi = 0.95$. The corresponding Flory–Huggins parameter for $\chi_{\mathrm{c}} = 5.52$ is calculated from Eq. (17) as 0.086. We assume that the polymer segment inside the block occupies the same average volume in all conformations. So we set $\phi_{\mathrm{A}I}^{\mathrm{in}} = \phi_{\mathrm{A}L}^{\mathrm{in}} = \overline{\phi}_{\mathrm{A}}^{\mathrm{in}} = 0.3$. The parameter for the deviation from random walk, δ, is 3.

The PP was also studied by the random walk version (rw) bnSCF ($\delta = 1$) that allows the random walk development of the chain. In this approach, the bnSCF model can also describe the experimental results (i.e. practically, without introducing the disturbed walk parameter δ). But in this case a depletion layer appears and the predictions are very similar to the results from the old nSCF. The C_∞ is set 5.2 and the bending energy from Eqs. (27) and (28) is $\varepsilon_L = 0.17 k_{\mathrm{B}}T$. The Kuhn statistical segment from Eq. (18) is $l_{\mathrm{K}} = 9.65$ Å. The number of monomers per block is 3.77. The interaction

parameter between the PP and the good solvent is $\chi = 0.85$. The corresponding Flory–Huggins parameter between the PP and the good solvent for $\chi_c = 3.56$ is calculated as $\chi = 0.12$. Again we assume that the polymer segment inside the block occupies the same average volume in all conformations $\phi_{AI}^{in} = \phi_{AL}^{in} = \overline{\phi}_A^{in} = 0.37$.

3.2. PEO in good solvent

In order to compare our method with experiment we have also investigated a system that has been studied with NR by Currie et al. [24]. The system is already studied with nSCF in our recent work [30]. It consists of diblock copolymer polystyrene–poly(ethyl oxide) (PS–PEO). The block copolymers were dissolved in chloroform and deposited on a air–water interface. The smaller PS blocks anchor the copolymers to the interface. This system has been treated as a system of grafted chains.

Since the bonds C–O and C–C do not have the same length we map the PEO monomer onto an equivalent 'polyethylene trimmer'. This equivalent structure contains only single bonds, each with bond length of $l_b = 1.96$ Å and angle between the two successive bonds, θ_b, at 131°.

In the results produced by means of the nSCF method, we have assumed that the temperature of our system is 25 °C, which is the temperature at which experimental data [24] were collected. The mass density is 1.10 g/cm^3; found in Ref. [31]. The Flory segment estimated (Eq. (20)) as $l_F = 4.315$ Å, therefore the number of chemical (ethyl oxide) monomers in a Flory segment is 1.21. In previous work [30], the C_∞ was estimated to have low value, because the χ for the interaction between polymer and solvent was also low ($\chi = 0.12$). It was based on the choice ($\chi = 0$) for the same parameter presented in Ref. [24]. We correct our previous approach by setting $C_\infty = 5$ and $\chi = 0.4$ [6]. For this C_∞, and for $l_b = 1.96$ Å Eqs. (27) and (28) give $\varepsilon_L = 1.09 k_B T$. The Flory interaction parameter between the PEO and interface is $\chi = -1$ (the minus sign shows that there is a preference for the surface).

In the bnSCF the value of the characteristic ratio (C_∞) is set 3.8. So we calculate the bending energy as $\varepsilon_L = 0.58 k_B T$. This value of C_∞ is very close to the one given by the literature ($C_\infty = 4$) [32]. The Kuhn statistical segment from Eq. (18) is $l_K = 8.2$ Å. The number of monomers per block is 2.3. The interaction parameter between the PP and the good solvent is $\chi = 2.7$. The corresponding Flory–Huggins parameter for $\chi_c = 6.22$ is calculated through Eq. (17) as 0.21. The interaction parameter between the PEO and interface for the new method is −12.7 and the corresponding Flory–Huggins parameter estimated by Eq. (17), is −1. We assume that the volume fraction of the *I* conformation is lower than the volume fraction of the *L* conformation: $\phi_{AI}^{in} = 0.24$, $\phi_{AL}^{in} = 0.28$, $\overline{\phi}_A^{in} = 0.27$. This is justified by the fact that the monomer (in the *trans* conformation) has 0.81 Å width and 3.56 Å length. The assumption of density fluctuations is defended by the resulting volume fraction profile. Also the parameter for the deviation from random walk, δ, is 3.

3.3. PS in good solvent

In addition we have compared our method with experimental results from a system studied with NR by Kent et al. [25]. The system investigated consisted of Langmuir monolayers of highly asymmetric poly(dimethylsiloxane)–polystyrene (PDMS–PS) diblock copolymers on the interface of air–ethylbenzoate (EB). This is a system with the smaller PDMS blocks (physically) anchored to the interface creating Langmuir monolayers. In our computational model we treat this system as a system of grafted chains, as the anchoring energies are very large [30].

In the results produced by theoretical methods, we have assumed that the temperature of our system is 25 °C, which is the temperature at which experimental data were collected. We use a mass density of 1.0525 g/cm^3; a value derived from expressions, of the mass density as a function of the pressure and temperature, found in Ref. [31]. The Flory segment estimated as $l_F = 8.016$ Å, therefore the number of chemical (isoprene) monomers in a Flory segment is 3.14.

The value used in nSCF method for the characteristic ratio, C_∞, of the equivalent trimer was estimated to be 8.0 [30]. For this C_∞, the bending energy is $\varepsilon_L = 0.538 k_B T$. The interaction parameter between the PS and the good solvent is $\chi = 0.15$. We assume that the interaction energy with the surface is zero.

The characteristic ratio in bnSCF method, C_∞, is close to value that was chosen for nSCF and is set 8.5. For this C_∞, the bending energy is $\varepsilon_L = 0.663 k_B T$. The Kuhn statistical segment for length of the C–C bond 1.54 Å and angle between two consecutive C–C bonds 112° is given from Eq. (18) as $l_K = 15.79$ Å. The number of monomers per block is 6.18. The interaction parameter between the PS and the good solvent is $\chi = 1.04$. The corresponding Flory–Huggins parameter for $\chi_c = 7.52$ is calculated from Eq. (17) as 0.07. We assume that the polymer segment inside the block occupies the same average volume in all conformations. So we set $\phi_{AI}^{in} = \phi_{AL}^{in} = \overline{\phi}_A^{in} = 0.25$. The results for both versions (random and disturbed walk) were taken for the same parameters. The disturbed walk is described with a value for parameter δ equal to 2.5.

4. Results and discussion

In Fig. 1 we present results for surface (grafting) density $\sigma = 0.1$ nm^{-2}. Our investigation includes one monodisperse system with 1422 monomers and three bimodal systems where the size of the long chains and the total surface density is kept constant. For PP of this molecular weight and grafting density, polymeric brushes are present. The solid line shows the results from the bnSCF compared to the predictions (dash and dotted) of the nSCF. The main difference between the two results is that the new method does not depict any depletion layer. We consider it as an improvement compared to previous nSCF methods since no experimental results seem to agree with the appearance of such layer near the surface. This behavior of the bnSCF was attributed to the variation from the random walk that was introduced. As mentioned in Section 2.2, by building a chain with specific bond energies, we increase the uniformly

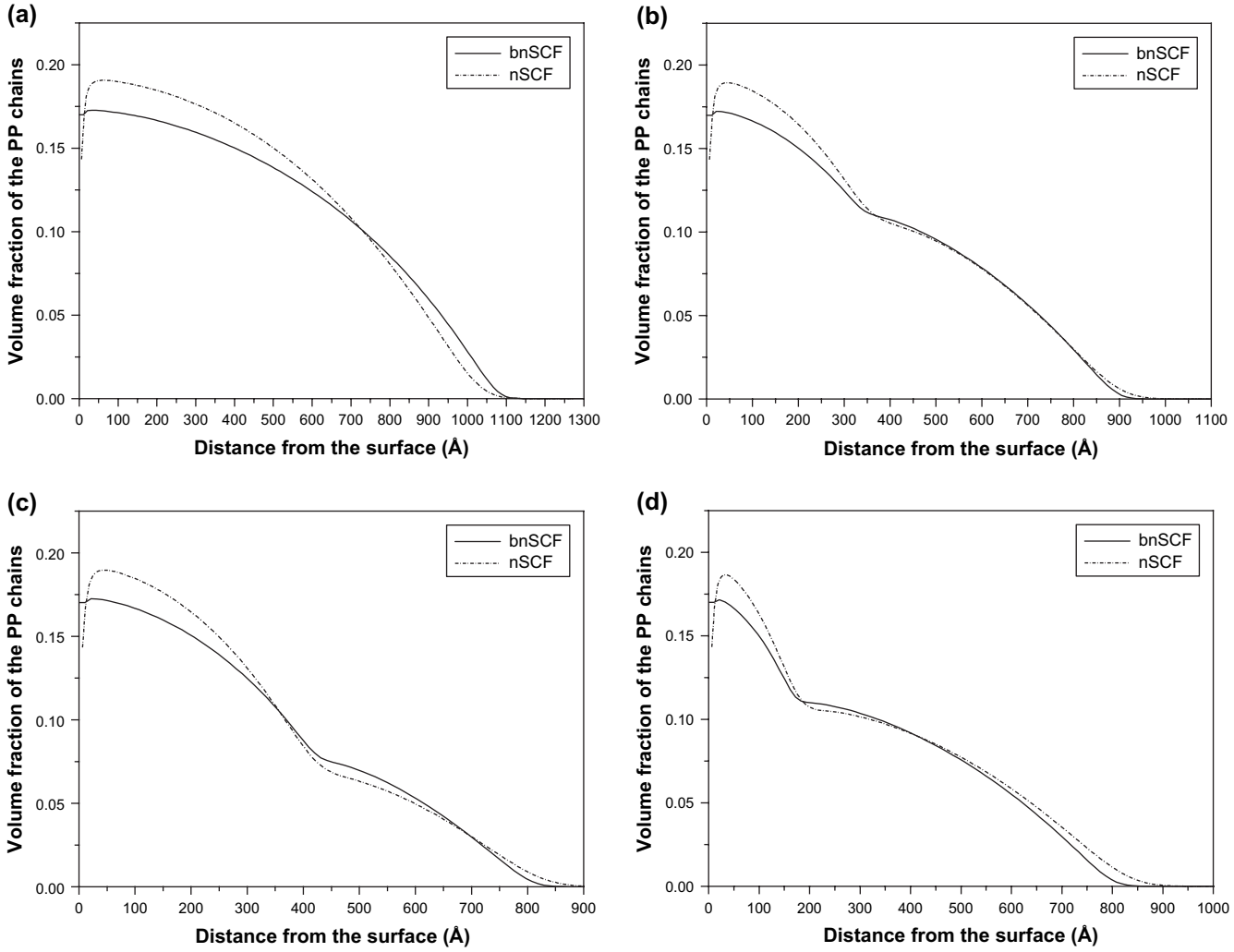

Fig. 1. Volume fraction profiles of PP chains as a function of the distance from the interface for one monodisperse and three bimodal systems. The dashed-dotted curve describes the prediction of nSCF model and the solid curve describes the prediction of bnSCF model. The systems studied are (a) 1422 monomers, $\sigma = 1 \times 10^{-1}$ chains/nm^2; (b) 1422-711 monomers, $\sigma = 1 \times 10^{-1}$ chains/nm^2, 60% short chains; (c) 1422-711 monomers, $\sigma = 1 \times 10^{-1}$ chains/nm^2, 80% short chains. (d) 1422-350 monomers, $\sigma = 1 \times 10^{-1}$ chains/nm^2, 60% short chains.

stretched configurations perpendicular to the surface (Scheme 2b). In this way mushroom-like conformations that distribute the chain in layers close to surface (Scheme 2a) have negligible contribution. The tendency to vanish the depletion layer with increasing surface density is also supported by investigations made with molecular simulations [33].

When the chains are intensely stretched using the disturbed walk development a reduction in the polymer concentration has much influence to the polymer configuration. In the bimodal distributions of Fig. 1 and also in Fig. 2 we present such cases. It is observed that the brushes shrink more in the new method compared to the old nSCF, where the conformations are more stable and less affected by the surface density. As will be shown in next paragraph this is in agreement with the experiment. The reason for this behavior is that we indirectly give more weight to the enthalpic factor. In the old method the entropic factor has been considered with more weight, which justifies their stability. This explanation is supported by the fact that when the chain growth through the block model follows the random walk approximation the shrinkage follows the old nSCF predictions. This is shown in Fig. 3 where we present results from the (rw) bnSCF. The polymer chain is mainly distributed to layers far from the surface and not ‘‘uniformly’’ (mushroom conformation) as done with the disturbed walk version. So the brush without having to fill the gap of the depletion layer, accomplishes the same extension with $C_\infty = 5.2$. The same C_∞ that gives good results for the brush region and the disturbed walk growth, also gives excellent agreement with the nSCF for lower surface densities using the random walk growth. This is shown for the case of PS solution in Fig. 6.

We now concentrate in the investigation of the PEO system. Although the old nSCF does not agree with the degree of the shrinkage, the experiment seems to follow the predictions of the bnSCF at least at high enough concentrations (brush region). In Figs. 4 and 5 we present results of bimodal brushes studied with NR. These results are also compared with the old method. In Fig. 4 the PEO brush shrinkage is more intense

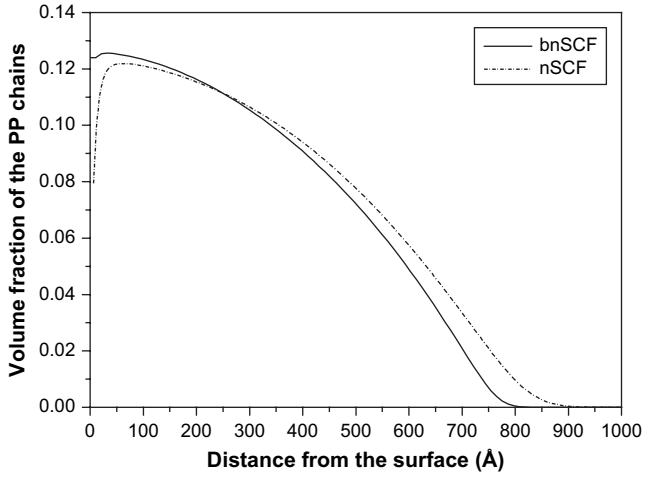

Fig. 2. Volume fraction profiles of PP chains as a function of the distance from the interface for monodisperse distribution and surface density lower than the previous cases, $\sigma = 0.5 \times 10^{-1}$ chains/nm^2. The number of monomers is 1422. The dashed-dotted curve describes the prediction of nSCF model and the solid curve describes the prediction of bnSCF model. The degree of shrinkage predicted by the new method is bigger than the one obtained from the old nSCF.

(bigger divergence from traditional nSCF) compared to the PS brush because the deviation from the random walk is bigger ($\delta^{\mathrm{PEO}} = 3$, $\delta^{\mathrm{PS}} = 2.5$).

In the study of the PEO system with the new approach assuming volume fluctuation for the I and L conformations, we observe that the first parabola of the bimodal profile became smaller taking lower values in the volume fraction profile. According to this estimation, the PEO monomer is rod like and when it is surrounded by water molecules, it is encaged in a smaller volume [34]. No important changes were

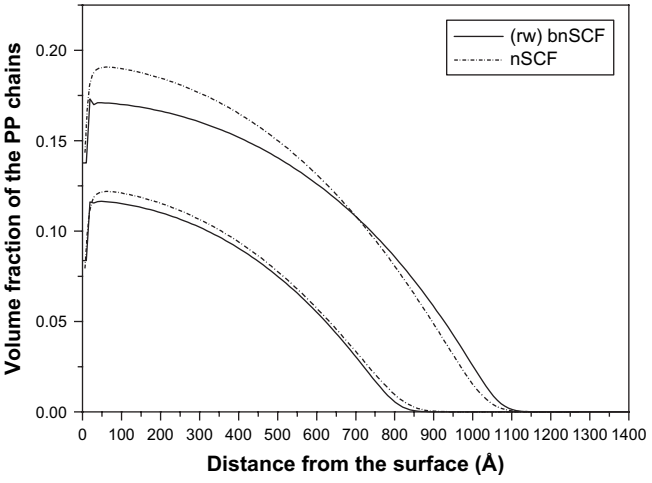

Fig. 3. Volume fraction profiles of PP chains as a function of the distance from the interface for two cases of monodisperse distribution. The surface density is $\sigma = 1 \times 10^{-1}$ chains/nm^2 and 0.5×10^{-1} chains/nm^2. The number of monomers is 1422. The stiffness of the chain for (rw) bnSCF method is 5.2 and it is smaller compared to the case where a variation of the random walk was introduced. The dashed-dotted curve describes the prediction of nSCF model and the solid curve describes the prediction of the (rw) bnSCF model. We observe that the results from the random walk version follow the predictions of the nSCF. The degree of shrinkage predicted by the new method is almost the same with the degree obtained from the old nSCF.

observed in the extension of the brush comparing to the case of constant volume for I and L segment conformations. This is attributed to the fact that at long distances from the surface the polymer volume fraction is low. Thereby the preference of the I block (in all three directions) in order to satisfy the enthalpic factor is strong only in small region near the surface. If we want to describe this solution using the traditional nSCF method, we have to consider a stiffer polymer than the predictions of the literature [32] (we set $C_\infty = 5$ instead of $C_\infty = 4$) and almost a θ-solvent ($\chi = 0.4$). In this way the polymer likes being close to the surface and since it is stiff it lies on the first layer. The part of the polymer on the first layer takes a rod-like conformation. This approximation explains the sudden reduction of the volume fraction observed in the NR experimental data. Of course if we accept that the I conformation occupies less volume, it becomes more preferable in the bnSCF method because the I block shows smaller interaction parameter ($\chi = \phi^{\mathrm{in}}_{\mathrm{AI}}\chi_{\mathrm{AB}}$). In this way it contributes to the reduction of enthalpic energy. So the increase of I angles is not succeeded only by lowering τ_L (when increasing C_∞). As a result we have good description of the system with low values of C_∞.

Finally, we study the PS system. In Fig. 6 we compare our method with PS results from NR [25] for three cases of bimodal distribution. It is obvious that the new method succeeded better description near the surface while the total extension of the brush predicted with the bnSCF method agrees with the experiment. A small deviation, compared to the old nSCF, occurs in the volume fraction value at point where the profile segregates in the two bimodal regions. Another choice of parameters in order to have better agreement on this point would slightly affect the volume fraction on the surface leaving the volume profile qualitatively unchanged.

In order to obtain a more accurate view about the region where the disturbed walk should be applied we have taken advantage of the experimental results for monodisperse PS layer height. In Fig. 6 we present results of the brush height as a function of ratio $\langle R^2\rangle^{1/2}/\sqrt{1/\pi\sigma}$. The $\langle R^2\rangle$ is given by Eq. (19) while the quantity $\sqrt{1/\pi\sigma}$ is characteristic of the free space that each polymer chain occupies in a brush of surface density σ and gives an estimate of the radius of that sector (R_σ). We observe that as the ratio becomes greater than 2 the disturbed walk version gives better results. The explanation of this behavior is the following. When the distance of the grafted points between two polymer chains ($2R_\sigma$) is greater than the double of end-to-end distance $2R$ (we assume $R \equiv \langle R^2\rangle^{1/2}$) then chains do not interact and we do not observe the brush phenomenon (Scheme 4a). As σ increases, the grafting points come closer. In Scheme 4b we describe the brush case where $R \le 2R_\sigma \le 2R$. In this case although the polymer's conformations (described with a hemisphere) interact, some configurations can still be developed with the random walk. The flatten conformations that end in the gray region are pushed perpendicular to the surface. So we have an extension of the brush which is owed to the fact that some conformations are stretched or others that follow the random walk get more weight. But in case where $2R_\sigma < R$ a chain that starts from a

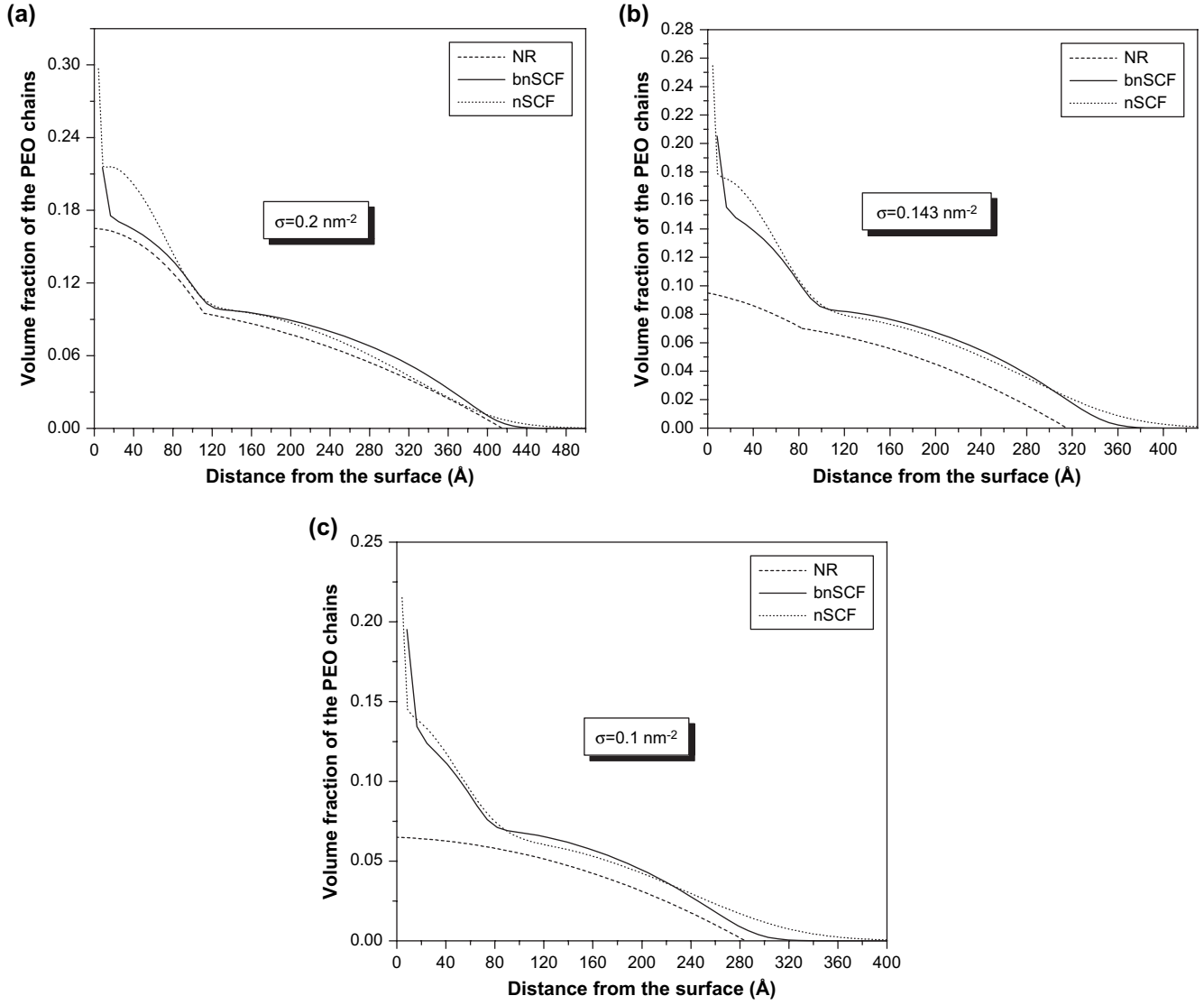

Fig. 4. Volume fraction profiles of PEO chains for bimodal distributions. The solid curve describes the prediction of bnSCF model, the dashed-dotted curve describes the prediction of nSCF model and the dashed curve the best fit to the experiment [24]. The bimodal systems studied contain chains with 700 and 150 monomers. The percentage of the short chains is 75. The Flory–Hugins parameter (χ) for the interaction between surface and polymer is -1 in both methods. We present three cases with three different surface densities (σ). (a) $\sigma = 0.2$ nm^{-2}, (b) $\sigma = 0.143$ nm^{-2} and (c) $\sigma = 0.1$ nm^{-2}.

grafting point on the surface cannot follow an undisturbed walk. In this case, the interaction with other chains is so strong that the brush is described using the disturbed walk version. The existence of three regions is supported by experimental results [35].

As shown in Fig. 6 for the cases where the ratio is lower than 2 the brush height is better described by the random walk version. For ratio value equal to 1 we do not have any experimental results so we have compared the new method with the old nSCF. It is shown that the rw versions of both nSCF methods (block and traditional) start from the same point (brush height) at low surface densities. Even when the ratio is greater than 2 but close to that value the random walk development is a better approach. When the ratio value is 2.2, the experimental data is almost the average value of the predictions of the two block versions (black and white triangle). In this case, the polymer chain is so long that even if a part of it is stretched there is still an important part that is described by the random walk development. The criterion for using the disturbed walk version is that R is much larger than $2R_\sigma$. In situation where the ratio is around 2, we should also consider the existence or not of the depletion layer in the volume fraction profile. The absence of such a layer is an indication of disturbed walk. The appropriate choice for each ratio value is marked with a gray circle. It is mentioned that we can always choose an appropriate (lower) stiffness parameter for the (rw) bnSCF version and describe the brush extension very well in all surface densities as done with the old nSCF. Only in this case we will observe even in high σ the appearance of the depletion layer near the surface (volume fraction profile).

If we try to transfer the disturbed walk in molecular simulation we should have the following approach. First let us assume that the interaction between two successive monomers on a chain or between two non-successive monomers of any

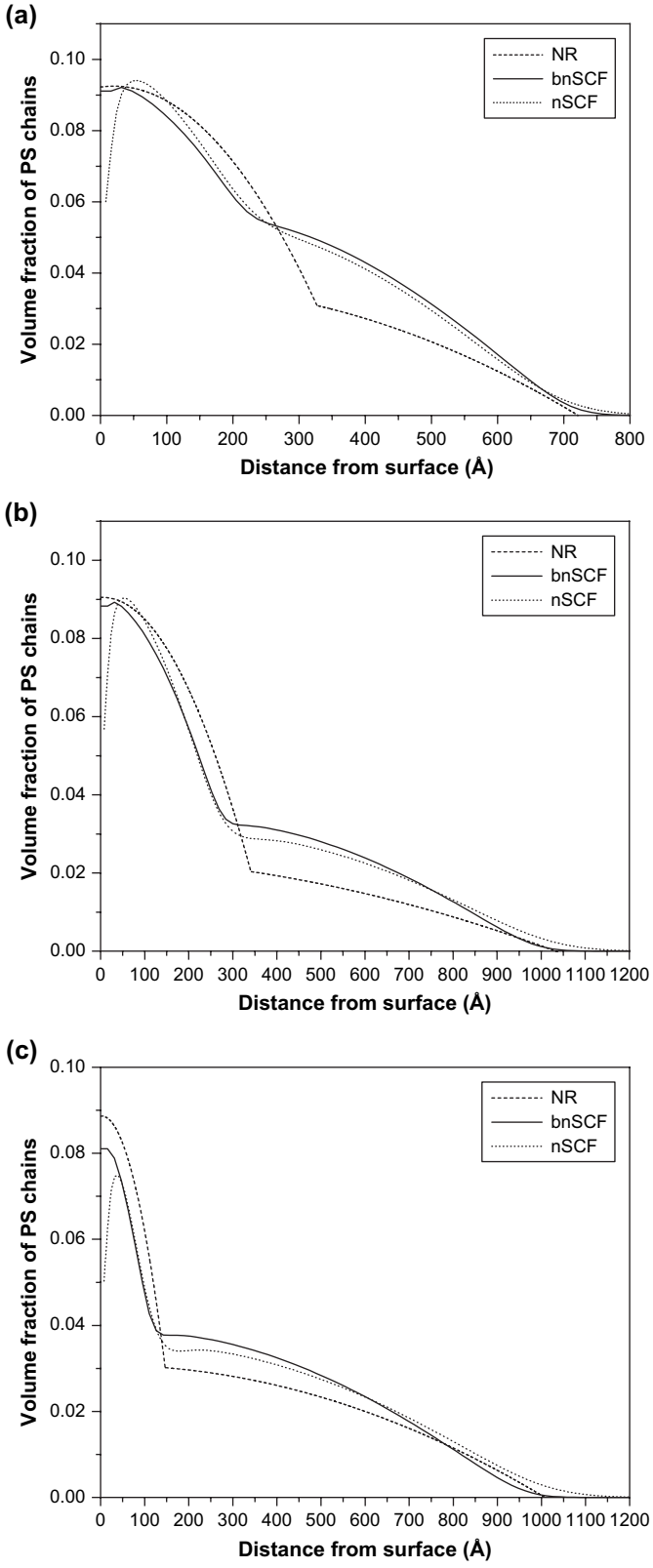

Fig. 5. Volume fraction profiles of PS chains as a function of the distance from the interface for three bimodal systems. The dashed curve describes the experimental result from NR, the dotted curve describes the prediction of nSCF model and the solid curve the prediction of bnSCF model. The systems studied are (a) 1634-634 monomers, $\sigma = 2 \times 10^{-2}$ chains/nm^2, 62% short chains; (b) 3173-634 monomers, $\sigma = 1.88 \times 10^{-2}$ chains/nm^2, 83% short chains; (c) 3173-288 monomers, $\sigma = 1.65 \times 10^{-2}$ chains/nm^2, 75% short chains.

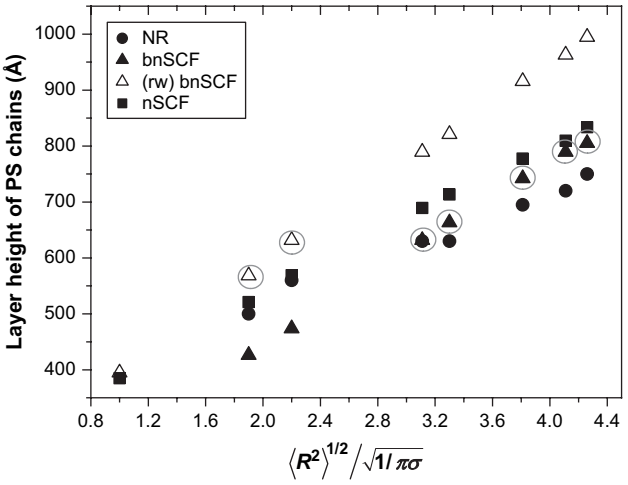

Fig. 6. Plot of the layer height as a function of the ratio $\langle R^2 \rangle^{1/2} / \sqrt{1/\pi\sigma}$. We study a system of monodisperse PS brush in various σ and we compare the predictions for the brush height from the bnSCF in the disturbed walk version (black triangles) and the random walk version (white triangles) with experimental results from NR (black circles) and theoretical results from previous nSCF method (black squares). The number of monomers is 1634 and $\langle R^2 \rangle^{1/2} = 181.10$ Å. We put in a gray circle the appropriate prediction (random or disturbed walk) for each ratio value from the new method. For ratio equal to 1 we present data only from the two theoretical methods because there was no experimental data.

chain is done with the use of hard spheres. Then we should consider different radius for each of the two different interactions. We accept that bond interaction has a smaller radius as it describes a stable bond. The hard sphere that occurs when the chain tries to move across the wall that is made by neighbor

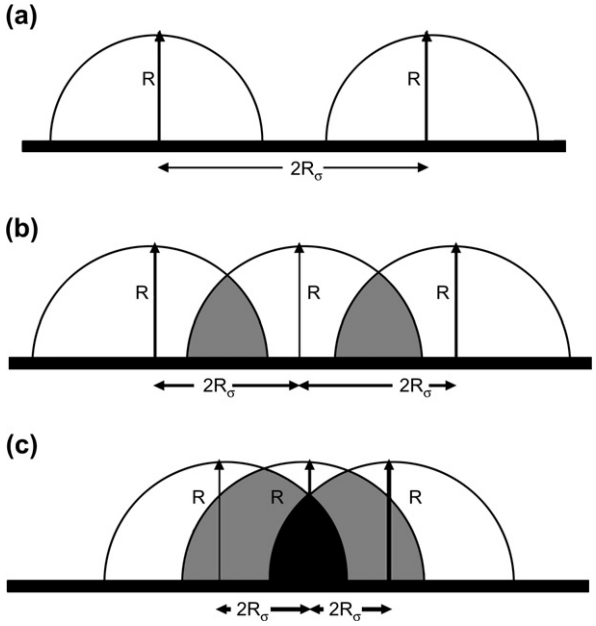

Scheme 4. Schematic with the three characteristic of regions of polymers grafted on surface. With R we present the end-to-end distance of a random walk development. The distance between two grafting points is $2R_\sigma$. All the possible conformations of a chain starting from a point on the surface and following a random walk development are described with a hemisphere of radius R. When two hemispheres overlap we have a gray area. The overlapping of three hemispheres is described with black. The three regions are the following: (a) $2R_\sigma > 2R$, (b) $R \leq 2R_\sigma \leq 2R$ and (c) $2R_\sigma < R$.

chains has a radius much bigger than the radius of a single bond. The reason is that as the double bond brings the atoms closer then it is reasonable to assume that the case of no bond should refer to a longer interatomic distance than the single bond. The result is that the chains at high concentrations cannot easily penetrate the wall of neighbor chains and so the chain has a difficulty to flatten parallel to surface and it stretches perpendicular to it. In this way we can observe the disappearance of the depletion layer.

By introducing the segment conformations inside the block, we make possible the atomistic study of the polymer molecule. The segment inside the block can be studied separately with accurate methods such as Monte Carlo. For one or more segments in the same block the energy and the internal volume fraction fluctuation could be defined using analytical potentials. In this way the mean field approach would be applied only for long distance interactions while a more detailed and refined estimation of the total energy of each conformation and the volume fraction profile could be achieved. Moreover because of the very good behavior near the surface, the bnSCF could be a powerful tool in order to study polymers very close to the surface (adsorption).

5. Conclusions

In this work we have presented a new approach for the study of polymer brushes through a revised nSCF method. The results of the new numerical method are very satisfactory since they improve the traditional numerical SCF method in the cases where the old method failed to follow the experiment. In some cases we have to introduce a new parameter that estimates the polymer stiffness in a more satisfactory way. We have found better results near the surface where we observe the disappearance of the depletion layer. We have also succeeded very satisfactory estimation of the brush extension as a function of the surface density. This method is an improvement of the old nSCF, with all the advantages of the old nSCF method, which is practically closer to a detailed atomistic approach without being as time consuming as an atomistic method.

Acknowledgements

This work was supported by the Greek Secretariat for Research and Technology (GGET) by a grant (PENED 03ED856).

References

[1] Alexander SJ. J Phys (Paris) 1976;38:977.
[2] DeGennes P-G. Macromolecules 1980;13:1069; DeGennes P-G. Scaling concepts in polymer physics. Cornell University Press; 1979.
[3] Milner ST, Witten TA, Cates ME. Macromolecules 1988;21:2610; Milner ST. Science 1991;252:905.
[4] Harpelin A, Tirrell M, Lodge TP. Adv Polym Sci 1992;100:31.
[5] Granick S. Polymers in confined environments. Berlin: Springer; 1999.
[6] Fleer GJ, Cohen Stuart MA, Scheutjens JM, Cosgrove T, Vincent B. Polymers at interfaces. Cambridge: Chapman and Hall; 1993.
[7] Auroy P, Auvray L, Leger L. J Phys Condens Matter 1990;2:317.
[8] Auroy P, Mir Y, Auvray L. Phys Rev Lett 1992;69:93.
[9] Taunton HJ, Toprakcioglu C, Fetters LJ, Klein J. Nature 1988;332:712.
[10] Taunton HJ, Toprakcioglu C, Fetters LJ, Klein J. Macromolecules 1990; 23:571.
[11] Klein J, Perahia D, Warburg S. Nature 1991;352:143.
[12] Tirrell M, Patel S, Hadziioannou G. Proc Natl Acad Sci USA 1987;84:4725.
[13] Ansarifar MA, Luckham PF. Polymer 1988;29:329.
[14] Taunton HJ, Toprakcioglu C, Klein J. Macromolecules 1988;21:3333.
[15] Cosgrove T, Heath T, van Lent B, Leermakers F, Scheutjens JM. Macromolecules 1988;20:1692.
[16] Patel SS, Tirrell M. Annu Rev Phys Chem 1989;40:597.
[17] Jones RAL, Richards RW. Polymers at surfaces and interfaces. Cambridge: Cambridge University Press; 1999.
[18] Retsos H, Terzis AF, Anastadiadis SH, Anastasopoulos DL, Toprakcioglu C, Theodorou DN, et al. Macromolecules 2002;35:1116.
[19] Mattice WL, Suter UW. Conformational theory of large molecules. New York: John Wiley & Sons; 1994.
[20] Scheutjens JM, Fleer GJ. J Phys Chem 1979;83:1619.
[21] Scheutjens JM, Fleer GJ. J Phys Chem 1980;84:178.
[22] Scheutjens JM, Fleer GJ. Macromolecules 1985;18:1882.
[23] Evers OA, Scheutjens JM, Fleer GJ. Macromolecules 1990;23:5221.
[24] Currie EPK, Wagemaker M, Stuart MAC, van Well AA. Macromolecules 1999;32:9041.
[25] Kent MS, Factor BJ, Satija S, Gallagher P, Smith GS. Macromolecules 1996;29:2843.
[26] Theodorou DN. Macromolecules 1988;21:1400.
[27] Wijmans CM, Leermakers FAM, Fleer GJ. J Chem Phys 1994;101:8214.
[28] Fischel LB, Theodorou DN. J Chem Soc Faraday Trans 1995;91:2381.
[29] Terzis AF, Theodorou DN, Stroeks A. Macromolecules 2000;31:1312; Terzis AF. Polymer 2002;43:2444.
[30] Kritikos G, Terzis AF. Polymer 2005;46:8355.
[31] Mark JE. Physical properties of polymers handbook. WoodBury, New York: American Institute of Physics Press; 1996; Brandrup J, Immergut EH. Polymer handbook. 3rd ed. New York: John Wiley & Sons; 1989.
[32] Gedde UlfW. Polymer physics. London: Chapman and Hall; 1996 [chapter 4].
[33] Daoulas KCh, Terzis AF, Mavrantzas VG. J Chem Phys 2002;116:11028.
[34] Kjellander R, Florin E. J Chem Soc Faraday Trans 1 1981;77:2053.
[35] Guangming L, Lifeng Y, Chen Xi, Guangzhao Z. Polymer 2006;47:3157.